Geosci. Model Dev. Discuss., 6, 1–35, 2013
www.geosci-model-dev-discuss.net/6/1/2013/
doi:10.5194/gmdd-6-1-2013

Geoscientific Model Development Discussions

Ice sheet dynamics within an Earth system model: coupling and first results on ice stability and ocean circulation

D. Barbi[1], G. Lohmann[1], K. Grosfeld[1], and M. Thoma[1,2]

[1]Alfred Wegener Institute for Polar and Marine Research, Bremerhaven, Germany
[2]Bavarian Academy of Sciences, Munich, Germany

Received: 10 December 2012 – Accepted: 17 December 2012 – Published: 7 January 2013

Correspondence to: D. Barbi (dirk.barbi@awi.de)

Published by Copernicus Publications on behalf of the European Geosciences Union.

Abstract

We present first results from a coupled model setup, consisting of a state-of-the-art ice sheet model (RIMBAY), and the community earth system model COSMOS. We show that special care has to be provided in order to ensure physical distributions of the forcings, as well as numeric stability of the involved models. We demonstrate that a statistical downscaling is crucial for ice sheet stability, especially for southern Greenland where surface temperature are close to the melting point. The simulated ice sheets are stable when forced with pre-industrial greenhouse gas parameters, with limits comparable with present day ice orography. A setup with high CO_2 level is used to demonstrate the effects of dynamic ice sheets compared to the standard parameterisation; the resulting changes on ocean circulation will also be discussed.

1 Motivation

For several decades, earth system models of growing complexity have been vastly utilized to study climate dynamics, and especially anthropogenic climate change (for a summary and comparison of recent results, see e.g. IPCC, 2007). These setups generally include models for atmosphere and ocean circulation, sea ice, and often also chemistry and vegetation modules. On the other hand, the large ice sheets are usually only represented by rule-of-thumb parametrizations. The reason for this neglections is that ice sheets are, under normal conditions, evolving on time scales much longer than atmosphere or ocean with maximum ice velocities in the order of magnitude of $1000\,\mathrm{m\,a^{-1}}$. Thus a separation of time scales seems to be in order.

When the climatic state to be studied is no longer at least quasi-static, this approximation becomes invalid. This is certainly the case for past climate eras of large-scale changes, e.g. glacial-interglacial transitions: deglaciation periods following ice ages can obviously not be simulated based on static ice sheets. In the palaeoclimate context, systems like the ocean and atmosphere have been parameterised or highly simplified.

GMDD
6, 1–35, 2013

But also the contribution of dynamic ice sheets on recent and future sea level rise needs to be addressed, as the IPCC (2007) points out: "Dynamics of the slow-moving ice and of ice shelves are reasonably well understood and can be modelled adequately, but this is not so for fast-moving ice streams and outlet glaciers. [...] Recent observations show that outlet glacier and ice stream speeds can change rapidly, for reasons that are still under investigation. Consequently, this assessment will not adequately quantify such effects." Breakup of buttressing ice shelves, acceleration of ice streams and outlet glaciers or drainage of the warming ice sheets are intensely argued upon. Indeed, satellite data as from the GRACE mission (Sasgen et al., 2012) give indications on accelerated mass loss in southern and western Greenland, in almost equal parts due to increased melting and draining glaciers. For a careful comparison to model results, a coupled setup of an earth system model to a 3-D-thermodynamical ice sheet model is mandatory.

Special care is needed concerning the spatial scales involved. While the atmosphere model was operated in low resolution (in the case of paleo-climate simulations T31 (3.75°)), the ice sheet model should not be run on grids coarser than 20 km. Consequently, the forcing data for the ice sheet, obtained from the atmosphere model, is too coarse to represent realistic distributions of temperature, accumulation or ablation. Our work shows that a careful downscaling procedure is mandatory to obtain stable ice sheet distributions, especially in southern Greenland.

2 Model descriptions

We shortly introduce the basic characteristics of the models we used, as far as they matter in the performed experiments. For any further information, we refer to the literature listed within the following paragraphs. The coupling scheme will be described in a later section.

GMDD
6, 1–35, 2013

2.1 RIMBAY

The 3-D-thermodynamical ice sheet model RIMBAY was first introduced by Pattyn (2003), and in recent years further developed by Thoma (Thoma et al., 2010, 2012). An important advantage of RIMBAY, compared to other ice sheet models, is the ability to integrate ice dynamics not only based on the standard approximations (Shallow Ice Approximation SIA, Shallow Shelf Approximation SSA), but also to higher order in the stresses (Full-Stokes). By definition of regions of interest, these integrations can also be combined: e.g. a fast-flowing stream can demand Full-Stokes, while in the surroundings, SIA can already be adequate. This feature makes RIMBAY effective and accurate in the same time.

Equally important is the implementation of moving margins, i.e. sheet-shelf-boundaries (grounding line), ice-ocean boundaries (shelf front) and ice-rock boundaries (nuntaks). These play a crucial role in the study of ocean feedback on shelves, which have been shown to possibly induce rapid shelf breakups (Hellmer et al., 2012; Determann et al., 2012).

2.1.1 Grid resolution, boundary and initial conditions

We used RIMBAY for independent simulations of Greenland and Antarctica ice sheets. For the boundary as well as initial values, we needed information about the geothermal heat fluxes, which we took from Shapiro and Ritzwoller (2004), as well as the bedrock topography and initial ice distributions. For Antarctica, the AlbMap compilation (Le Brocq et al., 2010) was used; in the case of Greenland, we worked with the bed topography and ice elevation data provided by Bamber et al. (2001). Both compilations provide a 5 km resolution, which we interpolated to a cartesian 20 km model grid as we found it to be sufficiently accurate for our purposes.

GMDD
6, 1–35, 2013

2.2 COSMOS

We utilize the comprehensive AOGCM ECHAM5-MPIOM without any flux corrections (e.g. Jungclaus et al., 2006). The atmosphere model ECHAM5 was used at T31 resolution ($\sim 3.75^{\circ}$) with 19 vertical levels. The ocean model MPIOM was run at an average resolution of $\sim 3^{\circ}$with 40 vertical layers, and has a high resolution around Greenland and Antarctica of up to 24 km. COSMOS has been intensely used for the study of very different aspects of climate sciences, notably for the production of IPCC scenario runs for AR4 and simulations covering the last millenium. Our version of COSMOS has been used for Holocene (Wei and Lohmann, 2012), glacial (Zhang et al., 2012), as well as Pliocene (Stepanek and Lohmann, 2012) and Miocene (Knorr et al., 2011) conditions.

2.2.1 Changes to ECHAM5 and grid resolution

The spectral atmosphere model ECHAM5 was operated in a T31 (3.75°) resolution, which is certainly very coarse, but still a good resolution for testing as technical problems regarding the coupling become more pronounced than on finer grids. As an example, we will show our downscaling procedure later in this work. With ECHAM5, we applied the HD-hydrology submodel (Hagemann and Dümenil, 1998) that routes runoff along fixed runoff masks which have to be prepared during preprocessing.

Major changes were already applied to the ice sheet mass balance parametrization of ECHAM/HD. Close inspection shows that ECHAM ice sheets are stable, meaning that the amount of water collected as snow/rain is exactly compensated by mass loss due to evaporation and runoff. We disabled this parametrization, now reading in ice orography from the ice model output. The mass budget routines for the HD-model were altered consistently. We furthermore included checks ensuring that both ECHAM5/HD and RIMBAY agreed on the mass balance of the ice sheets. No changes were applied to the MPI-OM ocean model, which we operated with a standard GR30 grid with shifted north pole over Greenland which provides a relatively high resolution around Greenland and Antarctica.

GMDD
6, 1–35, 2013

2.2.2 Initial and boundary conditions

The initial state of our integrations was taken from the results from a 800-yr equilibration run, which was forced with pre-industrial greenhouse gas concentrations (Wei et al., 2012; Wei and Lohmann, 2012). The initial state of the COSMOS-part of our setup is thus comparable to a pre-industrial climate. As the inital sheet ice distribution is taken from present-day data, we expect the coupled system to be out of equilibrum, and to reach a steady state only after an initialisation phase. This can indeed be observed, and will be shown later.

In two sets of experiments, we applied two different values for the CO_2-concentration, while keeping all other forcings identical to pre-industrial climate. The reference experiments were performed with a CO_2-concentration of 278 ppm. The results of these runs were analysed in order to validate long-time stablity of the climatic state. Using southern Greenland as an indicator, we developed an adequate statistical downscaling so that stability of ice sheets is ensured.

In a second phase, we used a high CO_2-level (999 ppm) to demonstrate the effect of ice dynamics in a scenario with large scale ice melt. We will compare the results to a standard COSMOS setup with parameterised, stable ice sheets.

3 Coupling scheme

3.1 Timing

Regarding the coupling of ice dynamics to atmosphere or ocean circulation, it is obvious that the processes under consideration are acting on very different timescales. The atmosphere, for example, is integrated using time steps of seconds, while an ice sheet will react to changing forcing only in the range of decades or centuries. This naturally led to the paradigm that ice sheets are at least quasi-stable, and not needed to be simulated at all.

The separation of time scales enables us to couple the models iteratively, meaning that we run the coupled atmosphere-ocean setup with prescribed ice boundaries, alternating with ice shield runs with fixed atmospheric forcings. The forcings and boundaries are updated depending on the coupling mode:

– Synchronous (transient) coupling:

  When in synchronous mode, both models are run iteratively, but in equal time steps, meaning after each period of atmosphere-ocean integation, we update the forcings to the ice sheets and simulate these for the same period, then transfer the changed ice orography and fresh water flows back to the global climate model. We chose the coupling period to be one year, as, for the time being, we neglect seasonal effects. The interest in smaller timesteps will rise once we include a direct coupling between ocean and shelf ice, and thus feedbacks from sea ice variations.

– Asynchronous coupling:

  While synchronous coupling is certainly the most intuitive way of coupling two models, it is nevertheless not applicable over very long integration times as these would require computation time beyond any reasonable limit. Luckily, as the (computationally expensive) atmosphere lives on time scales much smaller than the internal time scale of an ice sheet, we can choose different integration periods for both models. A sensible scheme would include a rather long integration period for the slowly changing ice sheets (1000 yr, e.g.), and a much smaller integration period for the atmosphere part, which we set to 25 yr which is sufficient for the atmosphere to adapt to the changed ice orography.

In both cases, we use the results of the last year of simulation as forcing for the next invocation of the other model. In asynchronous coupling, especially when a state of quasi-equilibrium is reached, it is advisable to exchange multiannual means instead, to compensate for interannual variability. As the only aim of the asynchronously coupled

GMDD
6, 1–35, 2013

runs within the scope of this paper is to demonstrate the existence of a stable state for the ice sheets, we could safely neglect these short-term effects.

3.2 Exchanged fields

The fields exchanged within each coupling timestep are presented in Table 1. In the center of attention lies the freshwater balance: The difference between net accumulation and ablation leads to changes of the ice thickness; ice moving across the sheet boundary is defined to be calved and returned, together with molten snow, to the ocean. The coupling scheme is conserving the total mass of the freshwater, which was ensured and controlled by testing routines within each model.

We also communicate annual mean and summer mean surface temperature to the ice model. Annual mean temperature is needed as boundary condition to the temperature distribution within the ice; summer mean temperature is needed during the downscaling process (see below).

Changed orography is returned as geopotential height, and albedo. Up to now, we did not change the land-sea-mask dynamically, which would be required for long-term paleoclimate applications.

3.3 Interpolation method

The basic interpolation was performed using a Shepard-algorithm; for a detailed discussion of as well as an implementation example see, e.g. Press et al. (2007). The Shepard-algorithm is a distance-weighting interpolation with weight functions of power-law type,

$$\frac{1}{d^e}, \tag{1}$$

where d denotes the distance between source and target grid point, and $e > 0$ is a choosable parameter, which we decided to set to 2.7.

GMDD
6, 1–35, 2013
Ice sheet dynamics within the Earth system
D. Barbi et al.

3.4 Downscaling

Already during the first tests, we had to see that the huge difference in resolution had a severe impact on stability of the Greenland ice sheet. This shall be illustrated by Fig. 1a – the map shows the ice sheet thickness after 10 000 model years, under pre-industrial forcing. It is clearly visible that southern Greenland is predicted to experience a rapid melt down. The reason can be seen in Fig. 2a, showing the ablation field as interpolated from ECHAM5 to the ice sheet grid. The patchy structure resembles the ECHAM5-resolution, which was set to T31. To circumvent the unrealistic distribution of precipitation and surface melting, we established downscaling procedures for the coupled variables. Three fields need to be downscaled: Net snow accumulation (i.e. precipitation minus evaporation), snow melt, and surface temperature. As we redistribute the data from coarse to fine grid, we "generate" information, which has to be taken from basic theoretic and empirical assumptions.

All downscaling methods we employed have in common that mass/latent heat are conserved, in the following sense: we calculated the net mass fluxes for accumulation/ablation over the ice as returned by the atmosphere model, and ensured that, after the downscaling procedure, both models agree on this value. In the same way, assuming that heat capacity is constant throughout the model domain (a necessary simplification), we made sure that also the net sum of latent heat over the ice is the same within RIMBAY as in COSMOS.

Moreover, we perform a regionalized downscaling – for the downscaled value at a given grid point, only data from cells within a defined radius is considered. This is important, as we do not want to mix information concerning distinct regions of the ice sheet; we especially need to distinguish between northern and southern Greenland. The Antarctic ice sheet remains stable throughout all the tests we performed. This is most certainly the case because surface temperatures are in general far from the melting point, accumulation is concentrated on some regions close to the coastlines, and snow melt is virtually non-existent. Changes in forcing, if not dramatic, will thus

GMDD
6, 1–35, 2013
Ice sheet dynamics within the Earth system
D. Barbi et al.

not show in the ice thickness distribution. For reference, we display literature values for surface temperature and accumulation from Ettema et al. (2009), which were obtained by high-resolution (11 km) regional climate modeling simulations using the Regional Atmosphere Climate Model (RACMO2/GR) (van Meijgaard et al., 2008).

We compare the results for ice thickness to measurement data from the Bamber et al. (2001) data set. These ice elevation data were derived from ice-penetrating radar data collected in the 1970s and 1990s, and regridded to a resolution of 5 km.

3.4.1 Net ablation

The distribution of melting snow is difficult to estimate. It strongly depends on the amount of time during which the surface temperature is above the melting point. As we were able to obtain a downscaled, high-resolution distribution of surface temperature, it is straightforward to use a Positive-Degree-Day-Model (Clyde, 1931; Collins, 1934). In this model, one assumes that the seasonal cycle varies as a sine function. From the summer and annual means, one can derive the number of days with temperatures above melting point. We furthermore assume that the number of days, on which snow is melting, is directly proportional to the amount of snow melting at this location. From the constraint that overall ablation is conserved, we get the ablation pattern as seen in Fig. 2b.

The PDD model, compared to results from a calculation of fluxes from the atmosphere data, has the advantage of leading to ablation in regions where the mean temperature is below the melting point, due to the assumed sine-like seasonal cycle. A disadvantage though can be seen in Fig. 2: the predominant wind direction is neglected. We decided to keep the PDD model as including the wind directions and speeds would ultimately lead to nesting of a regional model, which was beyond the scope of this project.

GMDD
6, 1–35, 2013

3.4.2 Net snow accumulation

A suitable formulation for the downscaling of net snow accumulation is based on an empirical relationship between surface gradient and rain fall (explained in Fortuin and Oerlemans, 1990). Therefore we redistribute snow fall proportional to surface gradient. Within a box surrounding the grid point x, we search for the highest as well as the lowest absolute value of gradient δ_{min} and δ_{max} (neglecting directions), and for the highest/lowest value of accumulation α_{min}, α_{max}. If $\delta(x)$ is the absolute value of the gradient at x, we estimate the accumulation $\alpha(x)$ linearly as

$$\alpha(x) = \frac{\delta(x) - \delta_{\mathrm{min}}}{\delta_{\mathrm{max}} - \delta_{\mathrm{min}}} \cdot (\alpha_{\mathrm{max}} - \alpha_{\mathrm{min}}) + \alpha_{\mathrm{min}}. \tag{2}$$

The result is corrected globally by multiplication with a constant so that the total accumulation is conserved. The resulting accumulation pattern can be seen in Fig. 3b.

3.4.3 Temperature

Mean annual as well as summer mean temperature are downscaled similarly. This time, instead for the surface gradient, we go for surface elevation, assuming that it is colder on higher elevations than on lower. We tried the classical laps rate correction, but found that a linear redistribution completely analogous to the method described for accumulation gives rather better results. Calling the temperature T and surface elevation h, we thus use:

$$T(x) = \frac{h(x) - h_{\mathrm{min}}}{h_{\mathrm{max}} - h_{\mathrm{min}}} \cdot (T_{\mathrm{max}} - T_{\mathrm{min}}) + T_{\mathrm{min}}. \tag{3}$$

Again, we correct the result so that the global surface integral of temperature is conserved; if one assumes that heat capacity is constant (a simplification, of course), then heat is also conserved. Results are displayed in Fig. 4b.

GMDD
6, 1–35, 2013

4 Performed experiments

We conducted a series of experiments, first of all for testing the coupling scheme, and in a later stage for the analysis of changes in ocean circulation. An overview is presented in Table 2. A detailed description can be found in the following paragraphs.

4.1 Stability tests – experiments 1a/b and 2

Before the coupled system can be reliably operated, checks against drifts in observables are in order. These tests are supposed to indicate mistakes and invalid approximations in the numerical implementation. We decided to analyse global mean surface temperature as indicator for the GCM state, and ice sheet mass balance (both locally and summed) which, as will be shown in the next paragraph, led to a reassessment of our coupling strategy.

All tests were performed starting from present-day ice thickness distributions and a well-established, "stable" GCM-state, using pre-industrial orbital forcings. To be able to see substantial changes in the ice sheet, we had to operate the setup in asynchronous coupling mode (experiments 1a and b).

The more detailed values for ice sheet mass balance as well as surface temperature were then taken from a comparable, but transient run (2).

4.1.1 The need for downscaling – experiments 1a/b

Figure 1a shows the resulting ice distribution of experiment 1a, after 10 000 model years. Ice mass is lost dramatically in southern Greenland, much more than realistic under the chosen forcing.

As the resolutions of the grids differ by orders of magnitude (20 km for the ice sheets, 3.75° for ECHAM), we assumed that not the net sum of the exchanged fields, but their distribution is the cause of the ice sheet instability. The relevant forcing variables (net snow fall, snow melt and surface temperature) are given in Figs. 3a, 4a and 2a: the

Discussion Paper | Discussion Paper | Discussion Paper | Discussion Paper |

GMDD

6, 1–35, 2013

Ice sheet dynamics within the Earth system

D. Barbi et al.

diagrams show the forcings as they are seen by the ice sheet model, resulting from a simple interpolation from the ECHAM-grid. Most problematic is the snow ablation, Fig. 2a. Obviously the whole predicted mass loss is concentrated at the southern tip of Greenland, leading to the observed mass loss.

Figures 3b, 4b and 2b show the downscaled forcings, accumulation and surface temperature can directly be compared to measurement data (Bamber et al., 2001), Figs. 3c and 4c. The improvement compared to the unscaled forcings is clearly visible. In the case of ablation rates, detailed measurement data is not available; the reader may be referred to Fig. 2c (Ettema et al., 2009) for an estimate taken from model simulations. The distribution of the ablation rates in Fig. 2c clearly differs from the result of our downscaling procedure (Fig. 2b), especially with respect to the western coast. This is not surprising as heat is carried towards Greenland by winds mainly from the west, which we did not account for. Nevertheless, the downscaled ablation rates seem much better physically justifiable than the unscaled.

Indeed, Fig. 1b demonstrates that downscaling leads to a more stable Greenland ice sheet; again, we present the result of 10 000 model years of ice sheet simulation (exp. 1b). Our result is very similar to the measured ice thickness, Fig. 1, showing more ice in most places. This of course makes sense as we simulated under pre-industrial conditions, but compare to the present-day ice distribution.

4.1.2 Ice sheet mass balance – experiment 1b

We present the details of the mass balance for each ice sheet in Table 3. The first to note is that all values are within a reasonable range, and comparable to literature values. If we look more closely, we notice:

– Greenland:

  The details of Greenland mass balance speak for themselves. Mass loss is caused up to about 40 % by surface melting, and about 60 % by calving – values that are in the same range as GRACE results (Sasgen et al., 2012). The net mass balance is close to zero, meaning the ice sheet is stable. As this is the difference between two almost equally sized numbers, the relative error is huge.

– Antarctica:

Again, results are in general agreement with present-day measurement data, see e.g. Le Brocq et al. (2010). The net mass balance is small but negative, meaning that Antarctica is slightly unstable in this experiment. There are two main reasons contributing to this result. First, even after 10 000 model years, the Antarctic ice sheet has not reached equilibrium in the sense that initial disturbances of ice distribution did not have enough time yet to relax. The reason is not only the larger extent, but also the much lower temperature in Antarctica compared to Greenland, making the ice dynamics slower. Indeed, in the details of the run, we can observe a slow trend towards a stabilization of the ice. Second, the version of RIMBAY we used to perform these experiments parameterized ice shelves crudely, a drawback that shall be overcome by recent changes to the model code. This led to unrealistic ice thicknesses in the shelf regions. The cause of the loss of ice in Antarctica will be further analyzed as we investigate the details of shelf-sheet interaction.

4.1.3 Surface temperature – experiment 2

The change in global mean surface temperature of the coupled run (2) can be seen in Fig. 5. Apart from the first 70 yr at the beginning of the run (which can be interpreted as adaptation phase to the changed boundary conditions of the GCM) the temperature remains on the same level, without any visible drift. We see that the change in temperature due to ice sheet coupling is negligible during the integration period, and, moreover, the system seems to run into a statistically stable limit.

GMDD
6, 1–35, 2013

4.2 Ice dynamic feedback on ocean circulation (experiments 3a/b)

In the following, we present an analysis of the effect of the dynamic ice sheet model on the resulting ocean circulation, by inspection of the anomaly fields. We first mention prominent effects, and try to explain them in the end of this section. All results are taken as a mean over the last 10 yr out of 350 simulation years.

4.2.1 Ocean surface temperature anomaly

Figure 6 shows the anomaly of sea surface temperature at the end of the simulation run. We want to point out two crucial regions: first, it is obvious that in the vicinity of Greenland, the surface water is colder when a dynamic ice sheet is present, compared to the setup with prescribed ECHAM-ice sheets. On the other side of the globe, most water close to the Antarctic coastline warms up considerably. This is to be compared to the same variable at a depth of 150 m (Fig. 7). Again, close to Antarctica the water is warmer than in the standard setup, but at this depth, also the Greenland region warms up.

4.2.2 Seawater salinity anomaly

Figure 8 demonstrates the freshening of surface seawater near Greenland. This, of course, is by no means surprising as we predict Greenland melting instead of a fixed Greenland ice sheet, so additional freshwater runoff to the North Atlantic Ocean is the consequence.

4.2.3 Sea ice compactness anomaly

An interesting result concerns sea ice compactness, Fig. 9. We like to point out that in order to see any effect, we present the anomaly after 100 rather than 350 model years. After 350 yr, both models agree, virtually no sea ice will be left in the Northern Hemisphere as we force the atmosphere with 999 ppm CO_2. The results after 100 yr,

GMDD
6, 1–35, 2013

though, show a very clear pattern: while the sea ice is thicker within most parts of the northern polar region, we predict sea ice mass loss all along the Antarctic coast, except the Ross Shelf area.

4.2.4 Meridional overturning circulation (MOC) anomaly

For completeness, we also present the change in meriodional overturning circulation (Fig. 10). As would be expected, MOC is weakened, especially in the uppermost layers.

5 Discussion

We coupled the dynamic ice sheet model RIMBAY to the global ESM COSMOS. The results clearly demonstrate that a coupled setup is possible, and indeed provides important corrections to simulations with fixed ice sheets. The details of the implementation are, though, far from trivial. Concerning the coupling scheme, we tried synchronous as well as asynchronous coupling. Both methods have their benefits depending on the scenario under investigation. If one is interested in short-term simulations, e.g. IPCC-like scenarios and projections, especially if the ice sheet is far from an equilibrium state, a synchronous coupling with short exchange period (~ 1 yr) is the best choice. When it comes to long-term simulations, like stability tests, an asynchronous scheme is the only option available regarding the huge demand on resources imposed by the ESM. Regardless of the synchronization scheme, we used an offline coupling strategy, exchanging data between seperate calls of the models. This surely has its disadvantages – a parallel version would be faster, and, in the long run, also easier to maintain. In principle, it would be desirable to implement a e.g. MPI-parallel version where the ice sheet model runs on a seperate process. We decided against this option as at the time our project started, RIMBAY development was still rapidly evolving, and we tried to keep portation issues as small as possible. We are planning to reorganize our implementation for future projects accordingly.

GMDD
6, 1–35, 2013

As the spatial scales of the ESM and the ice sheet model are very different, we used a downscaling procedure to redistribute atmospheric forcing to RIMBAY. Our semi-empirical ansatz proved to be sufficient for the production of stable ice sheets comparable to present-day orographies. A refining of these methods would be interesting, especially when regions sensitive to climate disturbancies are to be studied (outlet glaciers, shelf breakup). E.g. the influence of wind speed and direction have been completely neglected so far. Robinson et al. (2010) studied the use of a simple regional energy-moisture balance model (REMBO) to downscale ERA40 reanalysis data for ice sheet forcing. While their model is still very basic (the authors themselves refer to it as a downscaling procedure rather than a regional climate model), it nevertheless is considerably more complex than our method, including a set of fitting parameters we were able to avoid. The inclusion of all relevant processes would ultimately lead to the nesting of a regional climate model, or a refinement of the global ESM, as is possible with LMDZ (Li, 1999). In the long run, this is also the route of development we will pursue, as it represents the most consistent approach, avoiding the introduction of additional assumptions and simplification. On the other hand, as we are mainly interested in long-term simulations of the global climate, as in paleo simulations, for the time being we can restrict our downscaling method to the most influential effects.

Our results on ocean circulation convincingly demonstrate the importance of ice sheet dynamics on the global climatic state. We will discuss the effects on Arctic and Antarctic Ocean seperately:

– Greenland:

  The decrease in surface salinity (Fig. 8) in the surroundings of Greenland obviously results from the melting ice sheet, compared to the ECHAM-parameterization with fixed ice sheets. An interesting, and of course often discussed effect can be seen in the temperature anomalies: while the sea surface temperature is predicted to fall considerably in the Iceland region (Fig. 6), it increases at lower levels, and all over the North Atlantic (Fig. 7), similar to the vertical seesaw observed, e.g. in Knorr and Lohmann (2007), Barker et al. (2009).

These two combined effects can be interpreted as a lowering of the warm waters coming from the Carribean Gulf, diverted by the less dense surface water freshened by Greenland melt water. In the end, this rather leads to a strengthening of sea ice at high latitudes, compared to the model results with static ice sheets (Fig. 9), and a weakening of the AMOC.

– Antarctica:

  On the other side of the globe, we observe rather the contrary behaviour. Antarctica does not experience any dramatic mass loss. While other regions (e.g. the ice streams leading to the shelves) are gaining thickness, we observe increased melting especially in West Antarctica. This may trigger a strengthening of the gyres in the South Atlantic Ocean, and thus of the transport of warm water masses towards the Antarctic coast, as can be seen in both Figs. 6 and 7. Consequently, the sea ice breaks up (Fig. 9). As already mentioned above, it will be in the focus of further investigations how much of this effect is due to the way the ice shelves were parameterized.

6 Conclusions

Scenarios of Global Earth System Models like COSMOS strongly depend on the included ice sheet models. It is possible to couple dynamic ice sheets into the ESM COSMOS, even though time and spatial scales of the involved dynamics differ strongly. We demonstrated that we can reproduce realistic and stable ice sheet orographies when forcing the coupled system with pre-industrial greenhouse gas concentrations. The ice elevation in Greenland resembles the ice sheet as observed today, being rather thicker in the centre (as would be expected).

The difference in spatial scales forces us to a careful downscaling procedure, as we have clearly shown. This is especially crucial in ice regions close to the melting point, where small changes in the temperature and/or ablation rates can lead to drastic

GMDD
6, 1–35, 2013

mass losses, as could be seen at the example of southern Greenland. Concerning the downscaling method, the surprising result is that a very basic procedure is sufficient to provide stable ice sheets. A more elaborate downscaling, e.g. a nested regional model, might have many advantages when small regions sensitive to climate change are investigated; within the context of long-term simulations of global climate, a semi-empirical scheme as presented here already leads to reliable results.

Instable ice sheets can have a strong impact on ocean circulation. We have shown that rapid melting can lead to a cooling (Greenland) or warming (Antarctica) of the surrounding oceans. The anomalies of temperature in different depths, as well as of the sea surface salinity, clearly points towards a sinking of the Gulf Stream due to freshening of Northern Atlantic surface waters. The warming of the Southern Ocean should be seen within the context of shelf ice breakup, as is described in a recent article (Hellmer et al., 2012). Correspondingly, sea ice extents are also heavily influenced, with a relative stabilization of the Artic sea ice.

Acknowledgements. The authors would like to thank Ralf Greve and Ingo Sasgen for helpful discussions.

Funding by the Helmholtz Climate Initiative REKLIM (Regional Climate Change), a joint research project of the Helmholtz Association of German research centres (HGF) is gratefully acknowledged.

References

Bamber, J. L., Layberry, R. L., and Gogenini, S. P.: A new ice thickness and bed data set for the Greenland ice sheet 1: measurement, data reduction, and errors, J. Geophys. Res., 106, 33773–33780, 2001. 4, 10, 13, 26

Bamber, J. L., Layberry, R. L., and Gogenini, S. P.: A new ice thickness and bed data set for the Greenland ice sheet 2: relationship between dynamics and basal topography, J. Geophys. Res., 106, 33781–33788, 2001.

Discussion Paper | Discussion Paper | Discussion Paper | Discussion Paper |

GMDD

6, 1–35, 2013

Ice sheet dynamics within the Earth system

D. Barbi et al.

Barker, S., Diz, P., Vautravers, M. J., Pike, J., Knorr, G., Hall, I. R., and Broecker, W. S.: Interhemispheric Atlantic seesaw response during the last deglaciation, Nature, 457, 1097–1102, doi:10.1038/nature07770, 2009. 17

Clyde, G. D.: Snow Melting Characteristics, Bulletin No. 231, Utah Agricultural Experiment Station, 231, 1–23, 1931. 10

Collins, E. H.: Relationship of degree-days above freezing to runoff, EOS T. Am. Geophys. Un., 624–629, 1934. 10

Determann, J., Thoma, M., Grosfeld, K., and Massmann, S.: Impact of ice-shelf basal melting on inland ice-sheet thickness: a model study, Ann. Glaciol., 53, 129–135, 2012. 4

Ettema, J., van den Broeke, M. R., van Meijgaard, E., van den Berg, W. J., Bamber, J. L., Box, J. E., and Bales, R. C.: Higher surface mass balance of the Greenland ice sheet revealed by high-resolution climate modeling, Geophys. Res. Lett., 36, L12501, doi:10.1029/2009GL038110, 2009. 10, 13, 27

Fortuin, J. P. F. and Oerlemans, J.: Parameterization of the annual surface temperature and mass balance of Antarctica, Ann. Glaciol., 14, 78–84, 1990. 11

Hagemann, S. and Dümenil, L.: Documentation for the Hydrological Discharge Model, Technical Report No. 17, Max-Plack-Institut für Meteorologie, Hamburg, Germany, 42 pp., 1998. 5

Hellmer, H. H., Kauker, F., Timmermann, R., Determann, J., and Rae, J.: 21st-century warming of a large Antarctic ice shelf cavity by a redirected coastal current, Nature, 485, 225–228, doi:10.1038/nature11064, 2012. 4, 19

IPCC: Climate Change 2007: The Physical Science Basis, Contribution of Working Group I to the Fourth Assessment Report of the Intergovernmental Panel on Climate Change, edited by: Solomon, S., Qin, D., Manning, M., Chen, Z., Marquis, M., Averyt, K. B., Tignor, M., and Miller, H. L., Cambridge University Press, Cambridge, UK and New York, NY, USA, 2007. 2, 3

Jungclaus, J. H., Keenlyside, N., Botzet, M., Haak, H., Luo, J. J., Latif, M., and Marotzke, J.,: Ocean circulation and tropical variability in the coupled model ECHAM5/MPI-OM, J. Climate, 19, 3952–3972, 2006.

Knorr, G. and Lohmann, G.: Rapid transitions in the Atlantic thermohaline circulation triggered by global warming and meltwater during the last deglaciation, Geochem. Geophys. Geosy., 8, Q12006, doi:10.1029/2007GC001604, 2007. 17

Knorr, G., Butzin, M., Micheels, A., and Lohmann, G.: A warm miocene climate at low atmospheric CO_2 levels, Geophys. Res. Lett., 38, L20701, doi:10.1029/2011GL048873, 2011. 5

Le Brocq, A. M., Payne, A. J., and Vieli, A.: An improved Antarctic dataset for high resolution numerical ice sheet models (ALBMAP v1), Earth Syst. Sci. Data, 2, 247–260, doi:10.5194/essd-2-247-2010, 2010. 4, 14

Li, Z.-X.: Ensemble atmospheric GCM simulation of climate interannual variability from 1979 to 1994, J. Climate, 12, 986–1001, 1999. 17

Marsland, S. J., Haak, H., Jungclaus, J. H., Latif, M., and Röske, F.: The Max-Planck-Institute global ocean/sea ice model with orthogonal curvilinear coordinates, Ocean Model., 4, 91–127, 2003.

Pattyn, F.: A new three-dimensional higher-order thermomechanical ice sheet model: basic sensitivity, ice stream development and ice flow across subglacial lakes, J. Geophys. Res.-Sol. Earth, 108, 2382, doi:10.1029/2002JB002329, 2003. 4

Press, W. H., Teukolsky, S. A., Vetterling, W. T., and Flannery, B. P.: Numerical Recipes – The Art of Scientific Computing, 3rd Edn., Cambridge University Press, Cambridge, UK, 2007. 8

Robinson, A., Calov, R., and Ganopolski, A.: An efficient regional energy-moisture balance model for simulation of the Greenland Ice Sheet response to climate change, The Cryosphere, 4, 129–144, doi:10.5194/tc-4-129-2010, 2010. 17

Roeckner, E., Bäuml, G., Bonaventura, L., Brokopf, R., Esch, M., Giorgetta, M., Hagemann, S., Kirchner, I., Kornblueh, L., Manzini, E., Rhodin, A., Schlese, U., Schulzweida, U., and Tompkins, A.: The Atmospheric General Circulation Model ECHAM5, Part 1: Model Description, Report No. 349, Max-Plack-Institut für Meteorologie, Hamburg, Germany, 2003.

Sasgen, I., Klemann, V., and Martinec, Z.: Towards the inversion of GRACE gravity fields for present-day ice-mass changes and glacial isostatic adjustment in North America and Greenland, J. Geodyn., 59–60, 49–63, doi:10.1016/j.jog.2012.03.004, 2012. 3, 13

Shapiro, N. M. and Ritzwoller, M. H.: Inferring surface heat flux distributions guided by a global seismis model: particular application to Antarctica, Earth Planet. Sc. Lett., 223, 213–224, 2004. 4

Stepanek, C. and Lohmann, G.: Modelling mid-Pliocene climate with COSMOS, Geosci. Model Dev., 5, 1221–1243, doi:10.5194/gmd-5-1221-2012, 2012. 5

Thoma, M., Grosfeld, K., Mayer, C., and Pattyn, F.: Interaction between ice sheet dynamics and subglacial lake circulation: a coupled modelling approach, The Cryosphere, 4, 1–12, doi:10.5194/tc-4-1-2010, 2010. 4

Thoma, M., Grosfeld, K., Barbi, D., Determann, J., and Pattyn, F.: The numerical ice sheet–ice shelf model RIMBAY, description and appliations, The Cryosphere, in preparation, 2012. 4

Valcke, S.: OASIS3 User Guide (prism_2-5), CERFACS Technical Report TR/CMGC/06/73, PRISM Report No. 3, Toulouse, France, 2006.

van Meijgaard, E., van Ulft, L. H., van den Berg, W. J., Bosveld, F. C., van den Hurk, B. J. J. M., Lenderink, G., and Siebesma, A. P.: The KNMI regional atmospheric climate model, version 2.1. KNMI Tech. Rep. 302, R. Neth. Meteorol. Inst., De Bilt, Netherlands, 2008. 10

Wei, W. and Lohmann, G.: Simulated Atlantic multidecadal oscillation during the Holocene, J. Climate, 25, 6989–7002, doi:10.1175/JCLI-D-11-00667.1, 2012. 5, 6

Wei, W., Lohmann, G., and Dima, M.: Distinct modes of internal variability in the Global Meridional Overturning Circulation associated to the Southern Hemisphere westerly winds, J. Phys. Oceanogr., 42, 785–801, doi:10.1175/JPO-D-11-038.1, 2012. 6

Zhang, X., Lohmann, G., Knorr, G., and Xu, X.: Two ocean states during the Last Glacial Maximum, Clim. Past Discuss., 8, 3015–3041, doi:10.5194/cpd-8-3015-2012, 2012. 5

GMDD

6, 1–35, 2013

Ice sheet dynamics within the Earth system

D. Barbi et al.

Title Page

Abstract | Introduction

Conclusions | References

Tables | Figures

◀ | ▶

◀ | ▶

Back | Close

Full Screen / Esc

Printer-friendly Version

Interactive Discussion

Table 1. Data exchanged in each coupling step, depending on the direction of coupling.

Ice → COSMOS	COSMOS → Ice
Calving Rate	Net Snow Accumulation
Geopotential Height	Net Ablation
Albedo	Annual Mean Surface Temperature
	Summer Mean Surface Temperature

GMDD

6, 1–35, 2013

Table 2. Overview over the performed experiments. All simulations started from the same initial data described in Sects. 2.1.1 and 2.2.2. Note that some do not include a coupled ice sheet, these were done for reference.

Exp. number	Coupled ice	Downscaling	Ice model years p. coupling Period	GCM model years p. coupling Period	nb. of coupling periods	CO_2 (ppm)
1a	Yes	No	1000	25	10	278
1b	Yes	Yes	1000	25	10	278
2	Yes	Yes	1	1	400	278
3a	Yes	Yes	1	1	350	999
3b	No	Yes	n.a.	1	350	999

GMDD
6, 1–35, 2013

GMDD
6, 1–35, 2013
Ice sheet dynamics within the Earth system
D. Barbi et al.

Table 3. Mass balance of the ice sheets. Model values were taken from experiment 1b, as means over the first 10 000 model years, and including their statistical variability. All values in $\mathrm{Gt\,a^{-1}}$.

Source	Accumulation	Calving	Ablation	Net
Greenland	1005 ± 71	-635 ± 98	-421 ± 45	-12 ± 66
Antarctica	2462 ± 73	-2602 ± 116	-103 ± 13	-243 ± 121

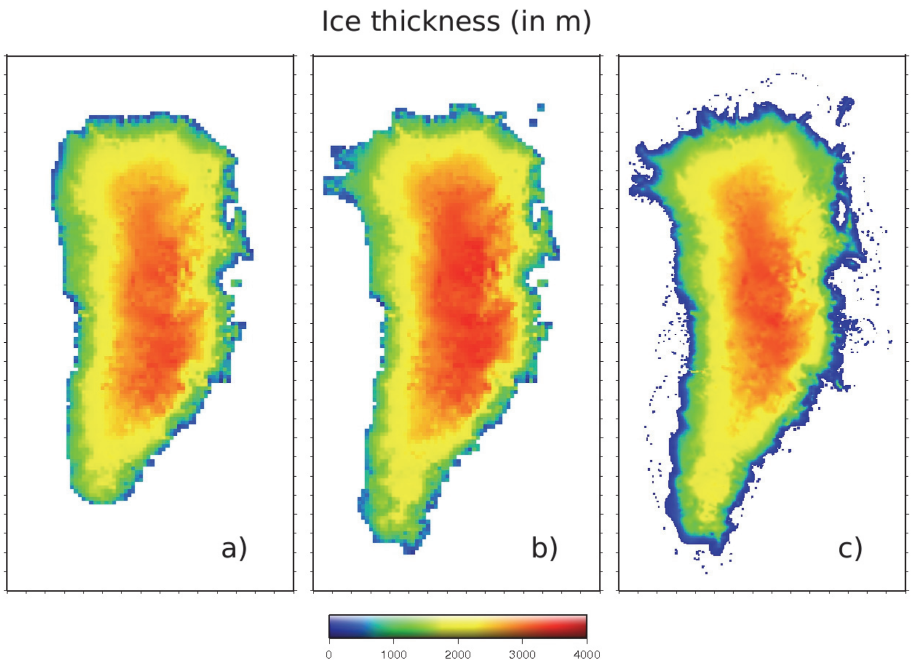

Fig. 1. Ice thickness of the Greenland ice sheet before (**a**, exp. 1a) and after (**b**, exp. 1b) the downscaling procedure, after 10 000 ice model years. This is compared to measurement data (**c**, Bamber et al., 2001).

GMDD
6, 1–35, 2013

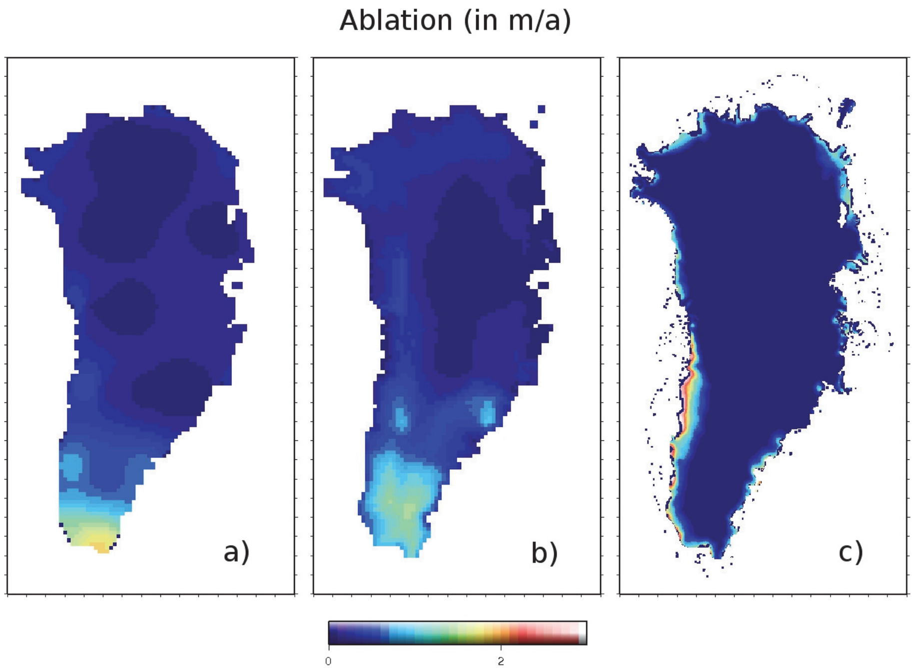

Fig. 2. Ablation pattern of the initial forcing over Greenland before (**a**, exp. 1a) and after (**b**, exp. 1b) the downscaling procedure. For reference, we also plot data from a regional climate model (**c**, Ettema et al., 2009).

GMDD
6, 1–35, 2013
Ice sheet dynamics within the Earth system
D. Barbi et al.

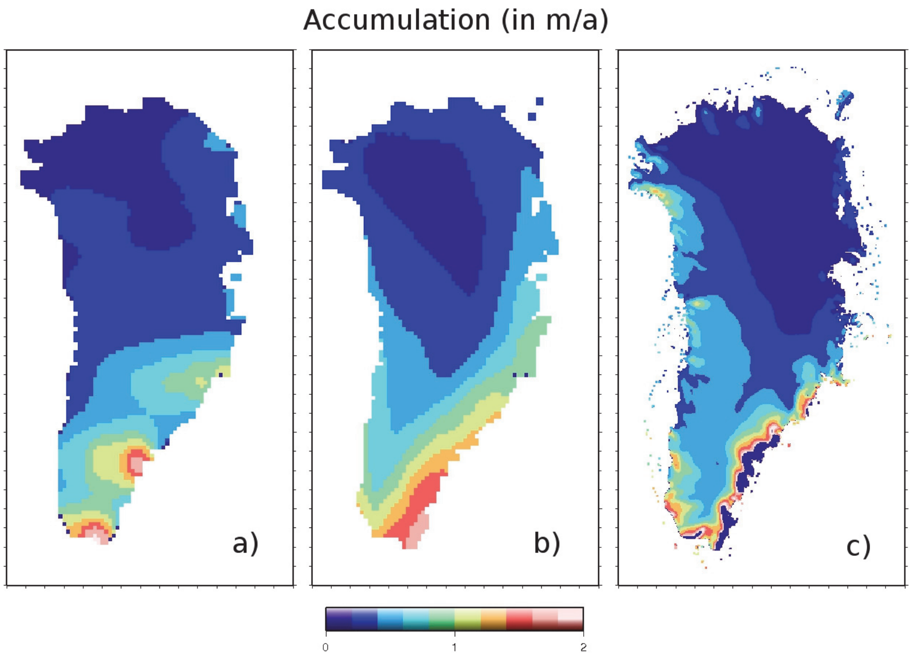

Fig. 3. As Fig. 2, but for accumulation rates.

GMDD
6, 1–35, 2013

Ice sheet dynamics within the Earth system

D. Barbi et al.

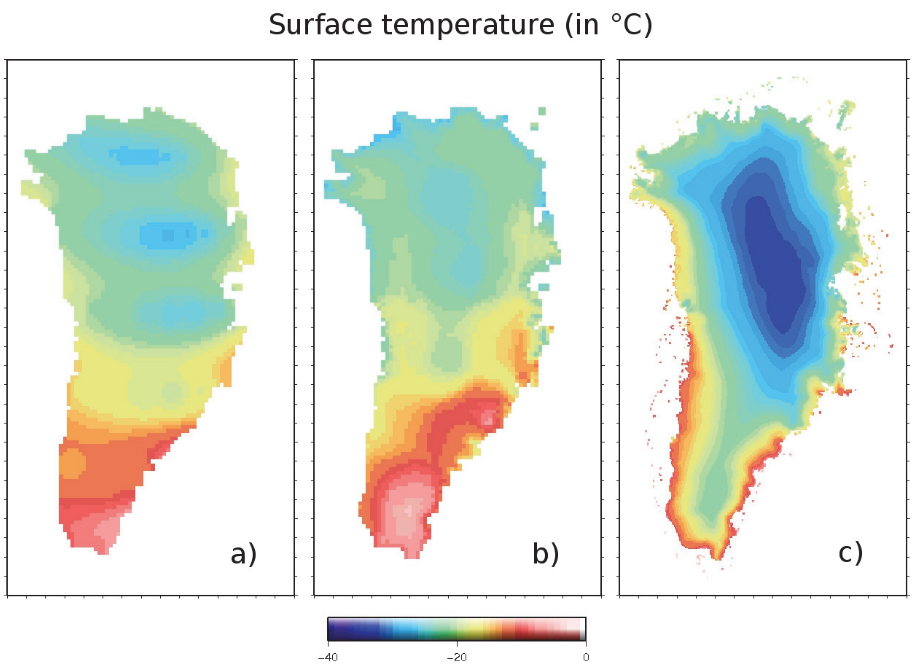

Fig. 4. As Fig. 2, but for surface temperature.

GMDD
6, 1–35, 2013

Ice sheet dynamics within the Earth system

D. Barbi et al.

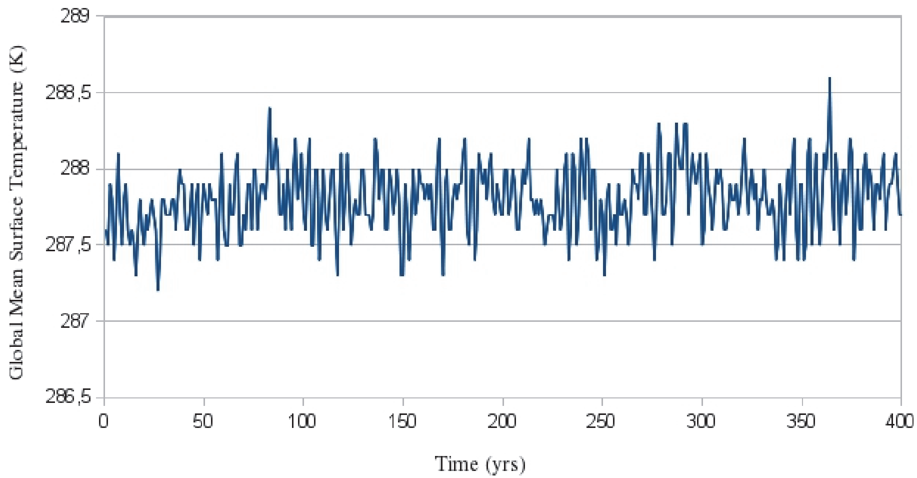

Fig. 5. Global mean surface temperature (K), from a transient 400-yr-run with pre-industrial greenhouse gas concentrations (exp. 2).

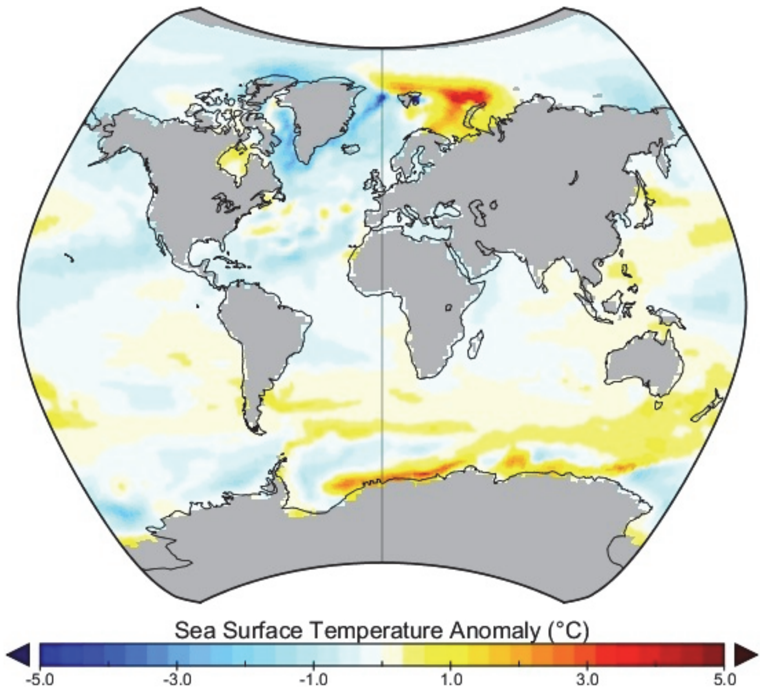

Fig. 6. Difference in sea surface temperature between experiments 3a and 3b, taken as a mean over the last 10 yr out of 350 yr of model simulation.

GMDD
6, 1–35, 2013

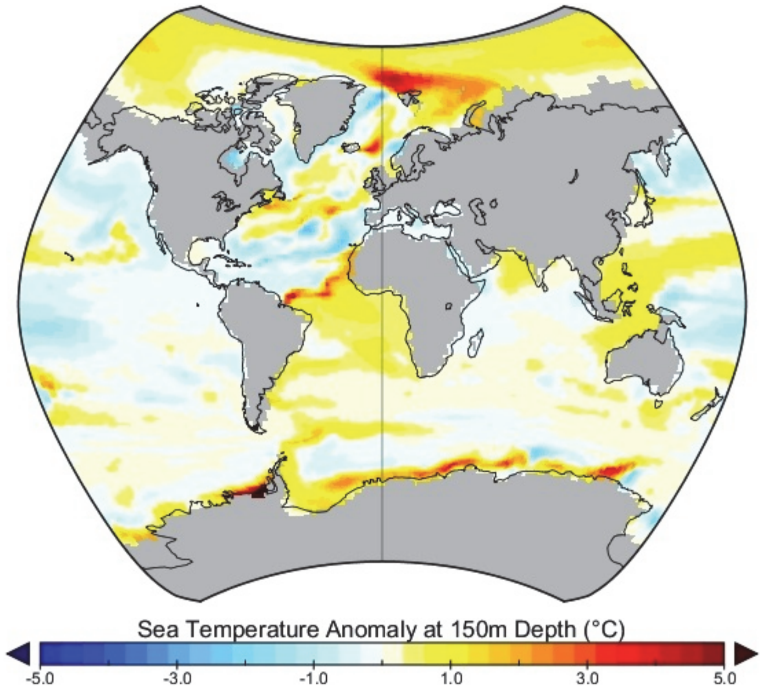

Fig. 7. As Fig. 6, but at 150 m depth.

GMDD
6, 1–35, 2013

Ice sheet dynamics within the Earth system

D. Barbi et al.

Title Page
Abstract Introduction
Conclusions References
Tables Figures
◂ ▸
Back Close
Full Screen / Esc
Printer-friendly Version
Interactive Discussion

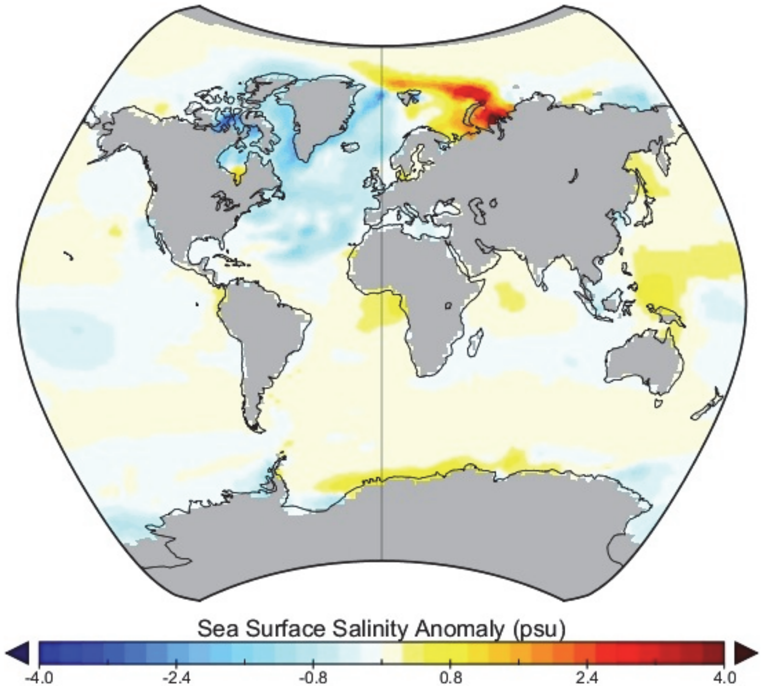

Fig. 8. As Fig. 6, but for seawater salinity.

GMDD

6, 1–35, 2013

Ice sheet dynamics within the Earth system

D. Barbi et al.

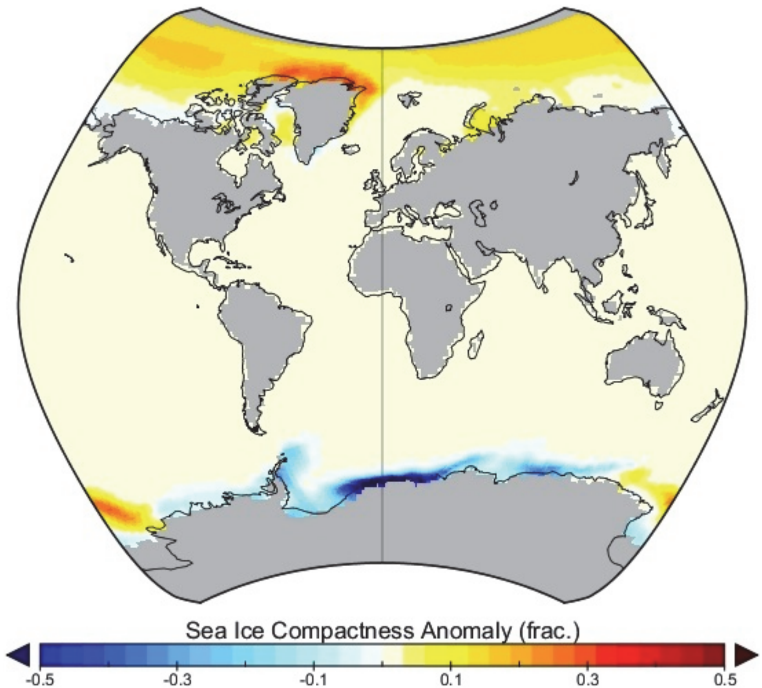

Fig. 9. Difference in sea ice compactness between experiments 3a and 3b, taken as a mean over the last 10 yr out of 100 yr of model simulation.

GMDD
6, 1–35, 2013

Ice sheet dynamics within the Earth system

D. Barbi et al.

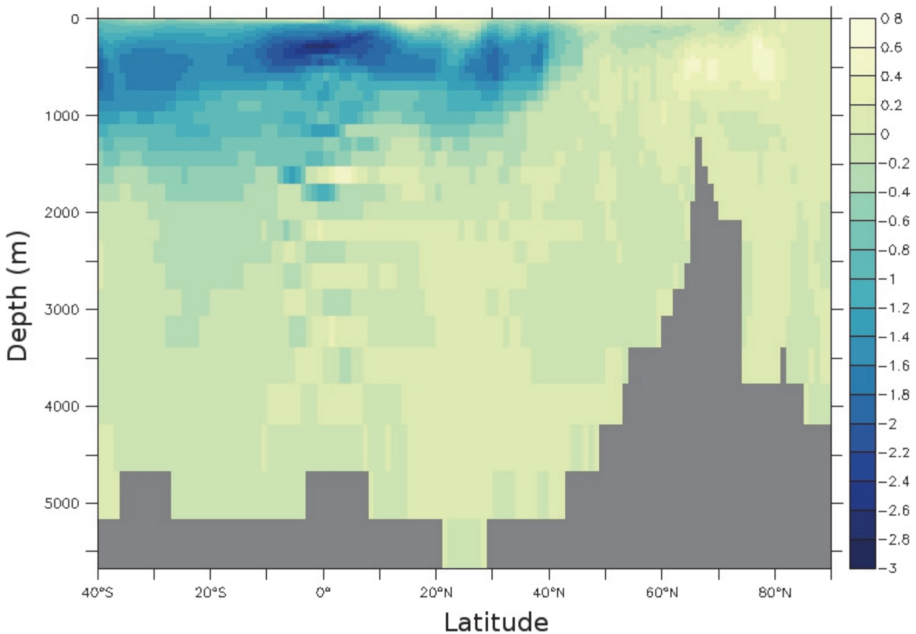

Fig. 10. Anomalous Atlantic Meridional Overturning Circulation (AMOC) between exp. 3a and b. Units are Sv = $10^6\ m^3\ s^{-1}$.

GMDD
6, 1–35, 2013

Ice sheet dynamics within the Earth system

D. Barbi et al.